Fed-Batch Droplet Nanobioreactor for Controlled Growth of Cyberlindnera (Pichia) jadinii
A Proof-Of-Concept Demonstration

Totlani, Kartik; Wang, Yen Chieh; Bisschops, Maxime; de Riese, Thorben; Kreutzer, Michiel T.; van Gulik, Walter M.; van Steijn, Volkert

Citation (APA)

Important note
To cite this publication, please use the final published version (if applicable).
Please check the document version above.

Fed-Batch Droplet Nanobioreactor for Controlled Growth of *Cyberlindnera (Pichia) jadinii*: A Proof-Of-Concept Demonstration

Kartik Totlani, Yen-Chieh Wang, Maxime Bisschops, Thorben de Riese, Michiel T. Kreutzer, Walter M. van Gulik, and Volkert van Steijn*

A key bottleneck in bioprocess development is that state-of-the-art tools used for screening of cells and optimization of cultivation conditions do not represent the conditions enforced at industrial scale. At industrial scale, cell growth is strictly controlled ("fed-batch") to optimize the metabolites produced by the cells. In contrast, cell growth is uncontrolled ("batch") in microwells commonly used for bioprocess development due to the difficulty to continuously supply minute amounts of nutrients to the cells in these wells over the course of the cultivation experiment. This work addresses this bottleneck through the development of a droplet-based fed-batch nanobioreactor. A key challenge addressed in this work is the implementation of the required non-steady droplet operations on chip to establish a semi-continuous nutrient supply, while keeping the chip and its operation as simple as possible. The ability to study micro-organisms under nutrient-controlled fed-batch conditions is demonstrated using the yeast *Cyberlindnera (Pichia) jadinii*, with the cell growth rate controlled through the glucose concentration. Given the relative ease of operation and the potential to extend its features, the presented nanobioreactor provides a solid platform technology for further development and use in the field of bioprocess development and beyond.

1. Introduction

Micro-organisms such as yeast and bacteria have the ability to naturally convert raw feedstock into useful products but often in amounts insufficient for industrial scale production.

K. Totlani, Y. Wang, T. de Riese, Prof. M. T. Kreutzer, Dr. V. van Steijn
Department of Chemical Engineering
Delft University of Technology
van der Maasweg 9, Delft 2629 HZ, The Netherlands
E-mail: v.vansteijn@tudelft.nl
M. Bisschops, Dr. W. M. van Gulik
Department of Biotechnology
Delft University of Technology
van der Maasweg 9, Delft 2629 HZ, The Netherlands

Improvement of the microorganism's product yield on feedstock is possible by targeted genetic modification, which requires a solid understanding of the species metabolism and genetics. Alternatively, genetic modifications can be introduced randomly such that the chance that a resulting mutant performs better than the original one is small. Consequently, many mutants need to be created and subsequently screened in order to identify the best performing ones.[1] Given the large number of experiments, it is common practice to grow and study all the different mutants in individual microliter-sized wells on microtiter plates. While this allows for parallel screening in an automated fashion using pipetting robots and plate readers, conventional microtiter plates lack the ability to feed nutrients and control pH by base or acid addition. It is indeed challenging to feed liquids at flow rates in the nanoliter per hour range to all the individual wells of a microtiter plate and to do so accurately. Therefore, screening of mutants is commonly performed under batch conditions with all feedstock present from the start and no further control over feedstock concentration and pH. In contrast, more than 80% of the processes in industrial biotechnology are operated under so called fed-batch conditions with control over feedstock concentration and pH.[2,3] This incompatibility between the physiological conditions during screening and industrial operation not only leads to selection of false positives which fail to generate competitive yields at industrial scale, but also fails to identify the best mutants for fed-batch conditions.[4–6] The effectiveness of screening hence greatly benefits from a technology that enables growing and studying a large number of microorganisms under precisely controlled conditions representative of industrial bioreactors. Besides screening of mutants, optimization of process conditions, a second important aspect in bioprocess development, also benefits from such a technology.[7] Although there has been progress in recent years, there remains both need and opportunity to cost-effectively and with fidelity miniaturize fermentation to screen under fed-batch conditions.

Several strategies have been developed to study microorganisms under controlled growth conditions. One strategy is to
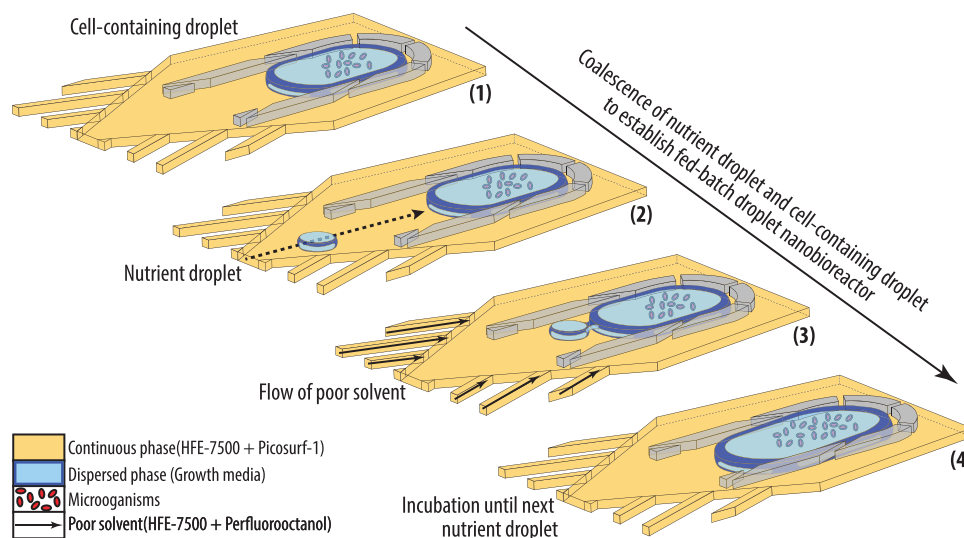
Figure 1. Conceptual schematic of the fed-batch droplet nanobioreactor illustrating the controlled supply of nutrients to a cell-containing droplet. Cell-containing droplet immobilized inside a cup-shaped trap (1). On-demand supply of a nutrient-containing droplet (2). Coalescence of the surfactant-stabilized interfaces induced by temporarily injecting a solvent in which the surfactant is less soluble through the fork-like structures (3). Incubation until the next nutrient supply (4).

improve existing platforms such as microtiter plates and shake flasks. Jeude and co-workers,[8] for example, implemented a continuous supply of glucose by adding glucose-containing silicon discs to shake flasks. A similar slow diffusive release strategy has been demonstrated in microtiter plates.[5,9,10] Scheidle and co-workers[5] used this strategy to compare the performance of 220 different mutants grown under batch conditions to that grown under fed-batch conditions, showing that best performers are not the same. Apart from slow release approaches, microchannels controlled through pneumatic valves have been added to or incorporated in microtiter plates for nutrient supply and pH regulation.[11–13] A second strategy is to integrate the wells and fluidic supply lines all in a single microfluidic device ,[14–19] see the comprehensive reviews by Grunberger's group. [20–22] A third strategy is to grow and study cells by compartmentalizing them inside aqueous microdroplets instead of inside solid wells.[23,24] This strategy may prevent issues arising in single phase microfluidic devices such as cross-contamination between the different wells due to lack of complete isolation and biofilm formation at the solid walls, but comes with its own challenges.[25–27] Microdroplets have been successfully used for screening of mutants where millions of droplets were encapsulated with cells and growth media at once, incubated off chip under batch conditions and reinjected in a separate chip to analyze and sort the best performing ones.[28–30] An outstanding challenge is to semi-continuously add nutrients to cell-containing droplets to perform screening under continuous or fed-batch conditions.[27,29]

Droplet-based assays that enable studies under controlled cell growth through controlled nutrient supply are scarce. Programmable devices have been developed[31–33] that could facilitate controlled microbial growth inside droplets that are spatially fixed on a chip, allowing sequential addition of nutrients by on-demand formation of nutrient-containing droplets, transport to the cell-containing droplets and induction of coalescence.

Jakiela and co-workers[34] as well as Jian and co-workers[35] in separate studies have used an alternative approach in which cell-containing droplets were circulated on chip and periodically flown through part of the circuit designed to split off part of the droplet and merge it with a nutrient droplet. While these studies successfully demonstrated cell growth studies under (semi) continuous conditions, the complexity of the devices and their use may prevent widespread adoption of this technology by the microfluidics community. Integrating long-term culturing in a controlled environment with accessible technology therefore still remains one of the great outstanding challenges in the field.[27]

In this work, we address this challenge by developing a nanobioreactor with a robust, yet simple nutrient supply strategy as also very recently demonstrated by Baroud's lab in the context of 3D spheroid formation,[36] eliminating the need for (on/off-chip) valves and optical feedback loops and allowing operation based on a single commercially available pressure pump. We present the first droplet-based nanobioreactor for cell studies under fed-batch conditions. While fed-batch is the most common mode of operation in industrial biotechnology, development of fed-batch chips so far receives surprisingly little attention from the microfluidics community.

2. Results and Discussion

2.1. Fed-Batch Droplet Nanobioreactor: Concept

The working principle of our fed-batch droplet nanobioreactor is illustrated in **Figure 1**. First, a cell-containing droplet is generated and trapped inside a cup-shaped trap (1). Being spatially fixed on the chip allows for easy monitoring of the growth of microorganisms. At will, a nutrient droplet is generated and flown into the trap (2). The challenge to coalesce the surfactant-stabilized interfaces is resolved by temporarily de-stabilizing the
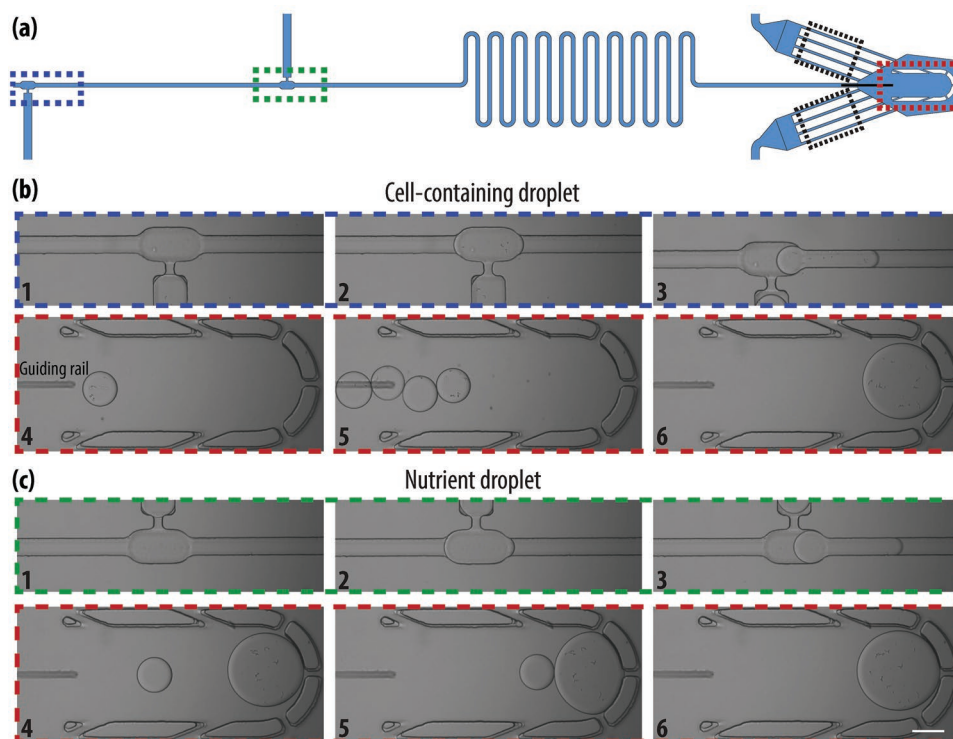
**ADVANCED
SCIENCE NEWS**
www.advancedsciencenews.com

**ADVANCED
MATERIALS
TECHNOLOGIES**
www.advmattechnol.de

Figure 2. Device design and operation of the fed-batch droplet nanobioreactor. a) Design showing a droplet on-demand junction for the generation of cell-containing droplets (blue box), a droplet on-demand junction for the generation of nutrient droplets (green box), a cup-shaped trap in which the cell-containing droplet is immobilized and studied under controlled growth conditions (red box), and two fork-like structures for the introduction of the solution with which coalescence is induced (black box) and a guiding rail (black line). To avoid back flow during injection of the poor solvent for coalescence or flushing, a serpentine channel is used between the DoD generators and the trap area to provide sufficient resistance. b) On-demand formation of a single cell-containing droplet (1–3) and its guidance into the trap through a guiding rail (4). Formation of a larger cell-containing droplet by sequential production of four droplets (5) and their coalescence (6). c) On-demand formation of a nutrient droplet (1–3) and its coalescence with the cell-containing droplet inside the trap (4–6). Scale bar is 100 μm.

interfaces by flowing a solvent around the droplets in which the surfactant is less soluble (3). After supplying fresh nutrients, cells are incubated and monitored until the next nutrient supply (4). This mode of operation, in which the cells are cultured under nutrient-controlled conditions, with the volume in which they are cultured increasing in time, is very common in industrial practice and better known as fed-batch operation. Unlike a chemostat, in which there is an inflow as well as an outflow, allowing it to run continuously, fed-batch processes have no outflow of effluent and run for a fixed time window. To enable the robust operation of the serial processes in the chip without the use of (on/off-chip) membrane valves or any active components on chip, we make use of the recently developed droplet on-demand generator.[37] Through the use of a single commercially available pressure pump, enabling facile adoption, we were able to establish the first example of a droplet-based nanobioreactor in which cells are studied under fed-batch conditions.

2.2. Fed-Batch Droplet Nanobioreactor: Device Architecture and Operation

Figure 2a illustrates the design, which features a droplet on-demand (DoD) junction for the generation of cell-containing droplets (blue box), a second DoD junction for the sequential

generation of nutrient droplets (green box), a cup-shaped trap in which the cell-containing droplet is immobilized and studied under controlled growth conditions through controlled supply of nutrient droplets (red box), and two fork-like structures for the injection of the solvent with which coalescence is induced (black box). Dimensions, fabrication protocols, and all other experimental details are provided in Section 4. The generation of a cell-containing droplet in oil is illustrated in Figure 2b. First, the interface between the aqueous cell solution and the oil is pushed against the nozzle of the DoD generator (Figure 2b1). Then, the pressure in the reservoir of the cell-containing solution is temporarily increased such that the interface is pushed through the nozzle and the chamber gets filled until it is full and the interfaces are pressed against the exits of the chamber (Figure 2b2). Finally, the pressure in the oil reservoir is temporarily raised to push the droplet from the chamber into the narrower main channel (Figure 2b3) and subsequently into the trap (Figure 2b4). The architecture of the DoD junction hereby allows for the production of a single droplet on-demand, with its volume set by the volume of the chamber, see Totlani et al.[37] for full details. To make sure that the droplet arrives in the trap, we make use of two features: a guiding rail in the form of a groove in the top wall between the exit of the main channel and the entrance of the trap and perforations in the cup-shaped trap that allow flow through the trap itself. Depending on the desired volume at the start of

**ADVANCED
SCIENCE NEWS**

www.advancedsciencenews.com

**ADVANCED
MATERIALS
TECHNOLOGIES**

www.advmattechnol.de

cultivation, multiple cell-containing droplets can be sequentially generated and pushed into the trap (Figure 2b5). Coalescence of these droplets is achieved by temporarily raising the pressure in the fluid reservoir that contains a solution in which the surfactant is less soluble, which is introduced in the area of the trap through the fork-like structures (Figure 2b6). Supply of nutrient droplets to the obtained cell-containing droplet follows a similar protocol, with the nutrients supplied from a separate reservoir and a second DoD junction as illustrated in Figure 2 c1–c6. For a given DoD geometry and a given nutrient concentration in the fluid reservoir, controlling the time interval between subsequent droplets (denoted as the waiting time (t_w)) is the most straightforward control over the nutrient supply rate. After each coalescence event, a residual flow of oil with surfactant is maintained via the main channel to ensure full wetting of the PDMS walls by the oil and stability of the cell-containing droplet during its incubation. After incubation, the cell-containing droplet can be extracted out of the chip for further analysis by reversing the oil flow which is possible by exchanging the outlet port with the inlet port for continuous phase. All operations are performed in an automated fashion using a MATLAB script that instructs a commercially available pressure pump with predefined pressure settings, see Supporting Information for script and settings. Using the here introduced approach, microorganisms can be studied under fed-batch conditions with their growth controlled through the controlled supply of nutrients.

2.3. Nutrient Feeding Profiles

The most straightforward cultivation method is the batch culture, wherein all nutrients are supplied at the start of the cultivation and the cells grow exponentially at their maximum rate until one of the medium components gets depleted. Controlling the supply of nutrients over the course of a cultivation experiment is important in biotechnological applications, because in this way the growth rate of the cells can be controlled and thereby also the rate of product formation. Because the relation between the rate of product formation and the growth rate can be different for each microorganism/product combination, a dedicated feed profile has to be designed to maximize the product formation rate and yield of a fed-batch process. Examples of basic feeding strategies are constant, linearly increasing and exponentially increasing feed rates, whereby the number of microorganisms increases respectively linearly, quadratically, and exponentially. Different feeding strategies can be established in the droplet fed-batch reactor by controlling the interval between subsequent nutrient supplies and the amount of nutrients fed per supply. Here we demonstrate constant and linearly increasing feed profiles. In case one nutrient-containing reservoir is used in combination with one DoD generator for the supply of nutrients, the nutrient concentration and the volume of a single nutrient droplet are fixed. Supply at a constant rate is then achieved by adding one nutrient droplet at a time at a constant time interval. An example of such a constant feed rate experiment is illustrated in **Figure 3**a, with the time interval equal to 10 min. One way to obtain a linearly increasing feed rate is to linearly decrease the time interval. Alternatively, the number of nutrient droplets per supply can be linearly
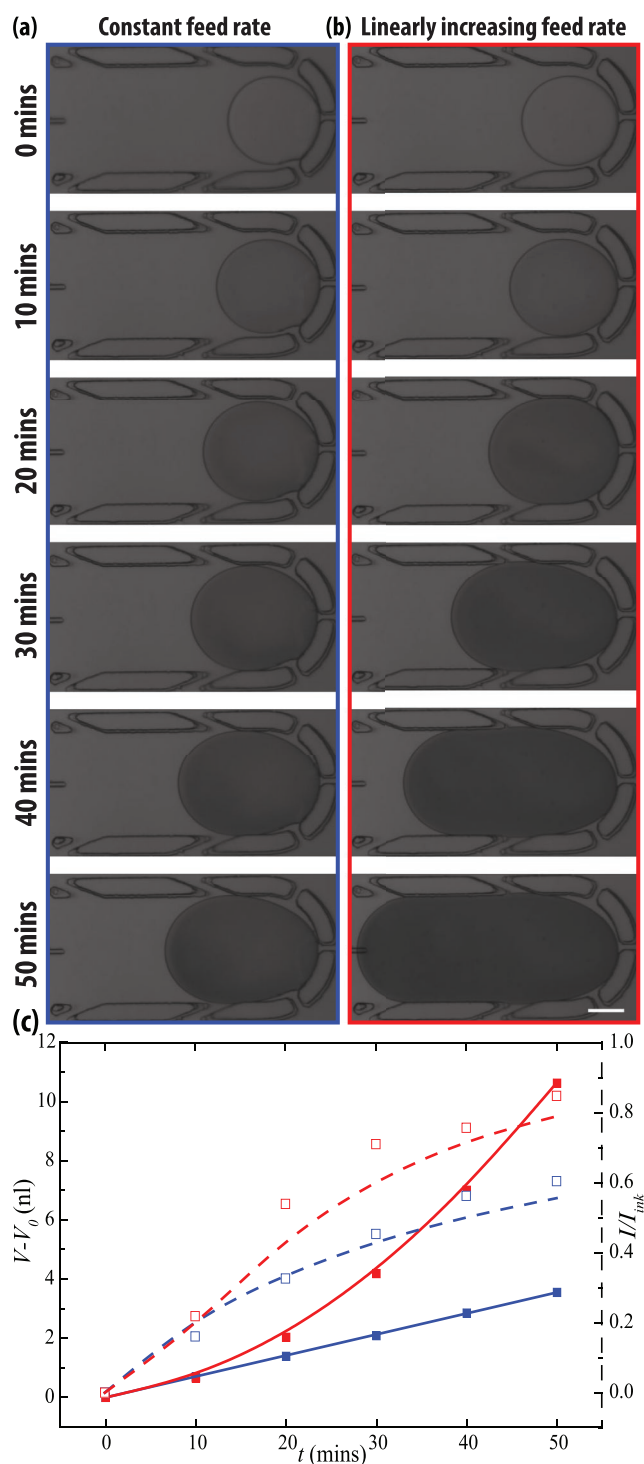

Figure 3. Demonstration of two basic nutrient-feeding strategies. For illustrative purposes and easy of quantification, we trapped an aqueous droplet and fed it with ink droplets. Gray scale images show the increase in volume and intensity of the trapped droplet for a) a constant feed rate (see the corresponding Movie S1, Supporting Information) and b) a linearly increasing feed rate. c) Corresponding volume of the trapped droplet V with respect to its initial volume V_0 (closed symbols) and gray levels I relative to that of an ink droplet I_{ink} (open symbols) agree well with theoretically expected values for volume (full lines) and relative intensity (dashed lines), see Section 4 for details. Scale bar is 100 µm.

**ADVANCED
SCIENCE NEWS**
www.advancedsciencenews.com

**ADVANCED
MATERIALS
TECHNOLOGIES**
www.advmattechnol.de

increased, while keeping the time interval between the supplies the same. An example of this mode of operation is illustrated in Figure 3b, with one droplet supplied after 10 min, two droplets shortly generated after each other (within 20 s) supplied after 20 min, and so on. The volume of the trapped droplet increases linearly and quadratically for a constant and linearly increasing feed rate respectively, as illustrated in Figure 3c. This increase agrees well with the expected increase based on the volume of the DoD chamber used to produce the droplets (0.71 nL). For illustrative purposes and ease of quantification, we performed these experiments by trapping an aqueous droplet and feeding it with ink droplets. This allowed us to straightforwardly verify that the concentration in the trapped droplet increases as expected through the measurement of the intensity, see Figure 3c. While the experiments presented here illustrate the working principle of the droplet nanobioreactor for two basic feeding strategies, we foresee that other, more complex, feed profiles are also possible. One limitation in establishing more complex feeding profiles arises from the frequency with which nutrient droplets can be generated. Two subsequent droplets can be generated within 20 s. In an exponential scheme, with 1, 2, 4, 8, 16, … nutrient droplets generated in subsequent supplies, the time it takes for the supply soon becomes comparable to the waiting time between the cycles. Another limitation arises from the volume of the trap relative to the volume of the chamber of the DoD generator, which currently dictates that 20 nutrient droplets can be fed until the trap is full. Potential improvements to overcome these two limitations are to incorporate multiple DoD generators connected to reservoirs with different nutrient concentrations, limiting the number of droplets that need to be generated per supply cycle. Using multiple reservoirs also opens up the possibility to supply basic/acidic solutions to control pH or other types of reagents, for example inhibitors, antibiotics, or even competitive microbial communities.

2.4. Controlled Growth of *Cyberlindnera (Pichia) Jadinii* in the Fed-Batch Droplet Nanobioreactor

After a successful demonstration of the ability to controllably produce and trap a cell-containing droplet and repeatedly supply it with fresh nutrients, we now show that we can utilize the developed approach to study cells under nutrient-controlled growth conditions. The model microorganism we used in this work is the Crabtree negative yeast *Cyberlindnera (Pichia) jadinii*, which was chosen for its relatively simple growth characteristics as it does not convert glucose to ethanol under aerobic conditions. Furthermore, its growth is severely limited under oxygen limited conditions[38] which allowed us to verify from the growth behavior whether oxygen limitation would occur. The experiments were designed such that glucose is the limiting nutrient with which cell growth can be controlled. To eliminate the need for active pH control over the course of the experiments, urea was used as the nitrogen source in the media. Based on these choices, cell growth is primarily controlled through the controlled supply of nutrients.

A typical cell growth experiment starts with overnight pre-cultivation in a shake flask and harvesting the cells in the exponential growth phase. Cells were washed with fresh defined medium to obtain a cell solution with a given initial glucose concentration C_{S0}. This solution was used to produce a cell-containing droplet, with the initial number of encapsulated cells (N_0) controlled through the washing step and the number of droplets used to form the cell-containing droplet. In our experiments, we used the protocol illustrated in Figure 2b and coalesced four cell-containing droplets of volume V_d resulting in an initial volume of $V_{m0} = 4V_d$. After cell handling and transfer to the microfluidic device, we first let the cells adjust to the environment for $t_b = 4$ h in order to verify that they continued their exponential growth. During this initial time window, which we refer to as batch phase-I, cells grew on the glucose present in the droplet without additional glucose being fed. The volume of the droplet remained the same, while the number of cells increased, as illustrated in the left column of **Figure 4**. After 4 h, we started the feeding phase in which we supplied nutrient droplets of volume V_d and glucose concentration $C_{S, in}$ at a constant supply rate characterized by a time interval t_w. The trapped droplet increased in volume during this phase, while the number of cells increased at a slower, nutrient-controlled rate, see the middle column of Figure 4. With the volume of the trap being almost 20 times larger than the volume of a single nutrient droplet (0.71 nL), 16 nutrient droplets could be fed to the cell-containing droplet over the course of the feeding phase. After this feeding phase, we continued monitoring cell growth up to 24 h, without further supply of nutrients, which we refer to as batch phase-II. During this phase, cell numbers increased at a reduced rate until the glucose is depleted, as illustrated in the right column of Figure 4. We observed moderate shrinkage of the trapped droplet during this phase, which is a well-studied phenomenon[39,40] with its dynamics governed by the evaporation of water through the PDMS matrix. To minimize shrinkage, the bonded chips were soaked in demineralized water for 7 days before the experiment and a stage top incubator with active humidity control was used during the experiments, see Section 4 for details.

The initial set of cell growth experiments we performed was designed in order to check that the protocol we developed, with all consecutive fluidic operations, does not itself influence cell growth. To this end, experiments without significant glucose limitation in the feeding phase were performed. The two parameters that control the extent of glucose limitation during batch phase-I are the initial cell number (N_0) and the initial glucose concentration in the cell-containing droplet (C_{S0}). The additional two parameters that determine the extent of glucose limitations from the feeding phase onward are the glucose concentration in the nutrient droplets ($C_{S, in}$), and the time between two subsequent nutrient supplies (t_w). Using a simple cell growth model (see Section 4) with estimates of the kinetic parameters from literature, we chose N_0 to be around 10 cells and $C_{S0} = 2$ g L^{-1} for cells to grow exponentially for the first 4 h and consume most of the glucose by the end of batch phase-I. This is indeed visible from the three growth curves in **Figure 5**. For the feeding phase, we chose three different glucose concentrations, $C_{S, in} = 0.1$, 1, and 5 g L^{-1} and a constant feeding rate with a time window of $t_w = 10$ min. For these parameters, the model predicted the cells to grow exponentially during the entire feeding phase and part of the subsequent batch phase without significant glucose limitation. The three curves
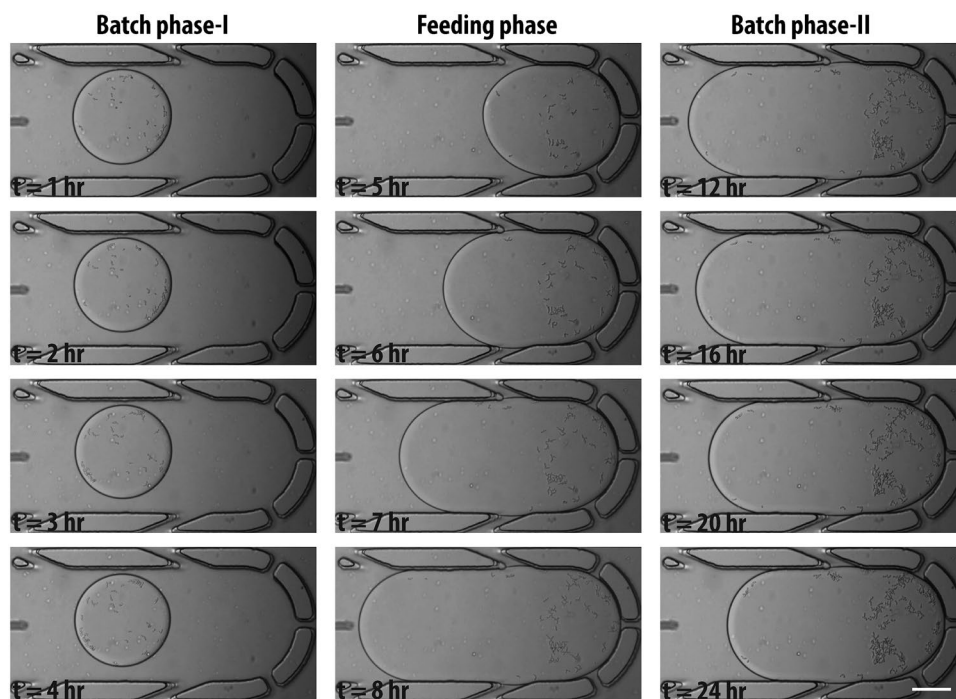
Batch phase-I	Feeding phase	Batch phase-II

Figure 4. Time lapse showing nutrient-controlled growth of *Cyberlindnera (Pichia) jadinii* inside a fed-batch droplet nanobioreactor. After cell handling and transfer to the device, cells were allowed to adjust to the new environment for 4 h, while growing on the glucose present in the trapped droplet. After this first batch phase (batch phase-I), the feeding phase started in which we controlled the cell growth through the controlled supply of nutrient droplets at a fixed rate (16 droplets with a time lag of 15 min). Once the trap was full, we continued monitoring cell growth up to 24 h while they again grew under batch conditions (batch phase-II). Scale bar is 100 µm. See the corresponding Movie S2, Supporting Information.

in Figure 5 indeed show the same (unrestricted) exponential growth. We obtained the specific growth rate by fitting the data in the initial and exponential growth phase. The specific growth rates are 0.28 ± 0.02 (5 g L^{-1}), 0.26 ± 0.01 (1 g L^{-1}), and
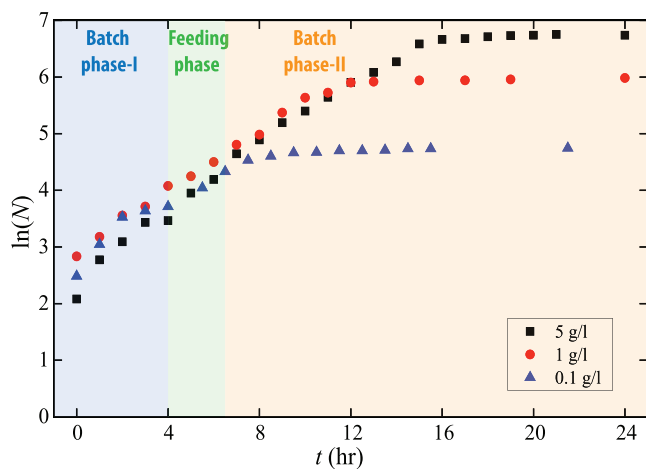

Figure 5. Growth curves obtained in the fed-batch droplet nanobioreactor under conditions without significant nutrient limitations. Comparable growth rates observed in the three different phases (as evident from the slopes) provide sanity check that the used protocol itself with all consecutive fluidic operations does not affect cell growth. Furthermore, similar growth rates observed for different glucose concentrations in the nutrient droplets, leading to different final number of cells, indicate that other limitations, such as oxygen, do not play a role.

0.24 ± 0.06 (0.1 g L^{-1}), with the ± values indicating the 95% confidence interval of the fitted values. The specific growth rates are not significantly different, illustrating the reproducibility of the experiments, and highlighting that the protocol itself does not affect cell growth. The rationale for performing the experiments at three different glucose concentrations in the nutrients droplets was to check whether other limitations, for example with regard to dissolved oxygen, played a role. The larger this concentration, the more cells were grown and the larger the rate at which nutrients were consumed. As the growth rate in the feeding phase and in part of batch phase-II is comparable for all three curves, we concluded that other limitations played no role for the studied parameter range. The order of magnitude of the final cell density is in the range 10^7– 10^8 cells mL^{-1}, which is comparable to the order of magnitude in traditional cultures.[41]

To demonstrate nutrient-controlled growth of *C. jadinii*, we chose appropriate values for the four main control parameters using the aforementioned simple cell growth model. While these parameters span a large window of operation for which nutrient-controlled growth is anticipated in the feeding phase, one of the most straightforward ways to control the extent of nutrient limitations is to simply start with a larger initial number of cells as compared to the previous set of experiments. This qualitatively results in a larger number of cells present in the cell-containing droplet at the start of the feeding phase and hence in a higher nutrient consumption rate, such that nutrient-controlled growth is anticipated when using comparable nutrient supply rates as in the previous set of experiments. Using the model, we quantified that an initial number
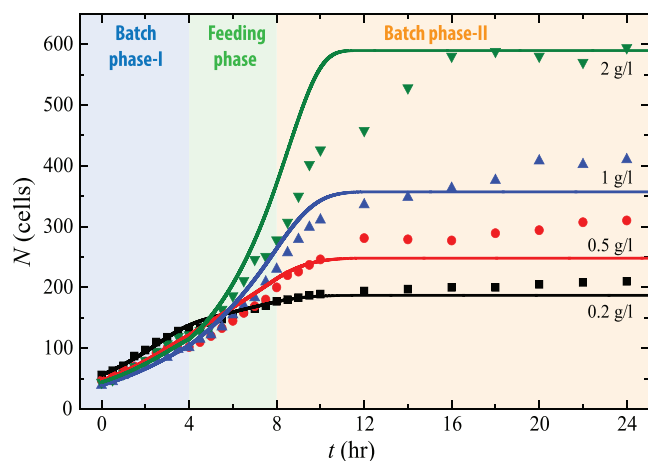
Figure 6. Growth curves for nutrient-controlled growth in the fed-batch droplet nanobioreactor. During batch phase-I all four experiments exhibit similar growth kinetics as the cell-containing droplets contain a common glucose concentration of $C_{S0} = 2$ g L^{-1}. The effect of controlled nutrient supply is seen from the difference in the growth rates in the feeding phase. Cell growth saturates at different final number of cells once the glucose gets depleted in batch phase-II. The experimental data (symbols) agree well with a simple cell growth model (lines).

of about 40 cells encapsulated in a droplet of volume 4 V_d with initial glucose concentration of 2 g L^{-1} gives rise to nutrient-limited growth with distinguishable growth rates when using glucose concentrations in the nutrient droplet of 0.2, 0.5, 1.0, and 2.0 g L^{-1} and a constant feeding rate of one nutrient droplet per 15 min.

The growth curves for these four controlled growth experiments are presented by the symbols in **Figure 6**. In batch phase-I, the conditions in the four experiments are comparable, except for the initial number of cells (between 39–56). The experiments are hence expected to show the same growth rate and can in this sense be seen as quadruplicates. The reproducibility of these experiments is evident from the overlap of the curves in batch phase-I in a plot with cell numbers normalized with the initial cell number and plotted logarithmically, see Figure S1, Supporting Information. In the feeding phase, the four experiments show a linear increase in the number of cells, characteristic for a constant supply of the growth limiting nutrient. Moreover, the slopes are significantly different, highlighting the ability of the here-developed nanobioreactor to control the growth of cells by the controlled supply of nutrients. After the feeding phase, the number of cells increases at a reduced rate in batch phase-II, with the final number of cells depending on the amount of glucose fed.

The controlled growth experiments were designed using a simple kinetic cell growth model, with estimates of the input parameters from literature. We can now compare model predictions with the experimentally-obtained growth curves. Rather than using the maximum growth rate (μ_{max}) and the yield on glucose ($Y_{x/s}$) as input parameters, we used them as fit parameters, as detailed in the Section S9, Supporting Information. As the yield on glucose is known to vary with the extent of nutrient limitation,[42] we fit it separately for batch phase-I and for the rest of the experiment. Despite the simplicity of the model, we obtained good agreement between model (lines) and experi-

mental data (symbols) for all the four variations of $C_{S, in}$ using a single set of fit parameters, see Figure 6. The obtained fit parameters are $\mu_{max} = 0.32$ h^{-1} and $Y_{X/S} = 0.35$ gX/gS (batch phase-I) and $Y_{X/S} = 0.45$ gX/gS (feeding phase and batch phase-II). These values seem lower than the range reported for *C. jadinii*,[43–45] which may be attributed to mixing. While the cell-containing droplet is mixed within 30 s each time coalescence is induced (Figure S2, Supporting Information), we observe limited motion of the cells inside the droplet. Mixing induced by the flow around the cell-containing droplet may be insufficient for effective mass transfer. Increasing this flow and optimizing the trap geometry enhances mixing and is subject for future development. Nevertheless, good agreement between model and experiments highlights the usefulness of this simple model, for the interpretation of nutrient-controlled growth experiments and for their design.

3. Conclusions and Outlook

The goal of this work was to develop a droplet-based nanobioreactor that enables studying microorganisms under nutrient-controlled fed-batch conditions as commonly encountered in industrial practice, but difficult to achieve at microscale with technology accessible to non-experts. To this end, we developed a robust method to controllably supply droplets with fresh nutrients to microorganisms encapsulated in a droplet immobilized in the nanobioreactor. We demonstrated the control over the growth of the yeast *C. jadinii* through the controlled supply of nutrients. A next challenge is to scale out the device in order to screen experimental conditions. In our previous work, we have shown the scale out of the droplet-on-demand junctions that form the foundation of the fed-batch chip.[37] A similar strategy can hence be used to scale out the fed-batch chip. Using DoD junctions with different chamber volumes in a parallelized architecture, it for example becomes possible to screen microbes for a variety of feeding profiles. A second challenge is to incorporate analytics to follow the production of intra- or extracellular metabolic products. Quantification of extracellular products secreted by microorganisms is possible by adding a third droplet on-demand junction that enables the addition of reagents to perform an end-point assay. Alternatively, real time fluorescence can also be measured during the fed-batch cultivation experiment, given the strain is engineered to express fluorescence. A third challenge is to further improve the accessibility of the technology. While the device itself is relatively simple and so is its operation through the use of a commercially available pressure pump, integrating and automating all workflows into a ready-to-use "chip-in-a-box"[46] is required to facilitate widespread adoption by biotechnologists and bioprocess engineers. All in all, given the ease of operation, the potential for scale out and incorporation of analytics, the presented droplet nanobioreactor provides a solid base for the screening of microorganisms or process conditions under industrially relevant fed-batch conditions. A benefit over microtiter-based fed-batch systems such as the BioLectorPro is the ability to perform these screens at single cell resolution and characterize cell heterogeneity.[46]

4. Experimental Section

Device Design and Dimensions: The most important features in the design of the microfluidic device as highlighted by the dotted rectangles in Figure 2a are: the two DoD generators for the production of the cell-containing droplet and the supply of nutrient droplets, the cup-shaped trap for the immobilization of the cell-containing droplet and the fork-like structures for the introduction of the solvent with which coalescence is induced. Full details on design considerations and performance (monodispersity) of the DoD generators are provided in our previous work.[37] The DoD generators consisted of a nozzle and a chamber. The nozzle was 25 µm wide, 25 µm high, and 50 µm long and connected to a 100 µm wide and 35 µm high supply channel. The chamber was 100 µm wide, 40 µm high, and 200 µm long resulting in a chamber volume of 0.71 nL. It was connected to the main channel, which was 50 µm wide and 35 µm high. The produced droplets were effectively guided from the exit of the main channel to the cup-shaped trap using a 20 µm wide and 5 µm deep groove in the ceiling of the channel. The trap was made up by a semi-circle with a diameter of 300 µm and a 300 µm wide and 900 µm long rectangle. The 30 µm wide and 35 µm high perforations in the trap hereby allowed flow through the trap. These perforations were not only important to load the trap with a droplet, but also to flush out unwanted bubbles or droplets produced at the start-up of the experiment. Their removal was achieved in a straightforward way by sufficiently raising the operating pressure in the reservoir from which the poor solvent was supplied, which forces them through the opening in the center of the trap into the downstream channel. The height of the trap was 35 µm, which was sufficiently shallow to avoid complications in cell counting due to the growth of cells in multiple layers for the growth conditions considered in this work. Coalescence between the immobilized cell-containing droplet and an incoming nutrient-droplet was achieved by introducing a poor solvent into the trap through the fork-like structures, which feature three channels that were 33 µm wide and 35 µm high. As coalescence was observed to occur within seconds upon the introduction of the poor solvent, these features were no subject for further optimization. The serpentine channel between the DoD generators and the trap area was added to provide sufficient resistance to avoid back flow when injecting the poor solvent into the chip during coalescence or flushing steps. The design and all its details were made available as an AutoCAD file in the Supporting Information.

Device Fabrication: Microfabrication was performed using standard photolithographic methods.[47] The device comprised channels of three different heights: all channels are 35 µm high, except for the 25 µm high nozzles, the 40 µm high chambers of the two DoD generators, and the 5 µm deep groove in the ceiling of the main channel. The 3D device was constructed from three layers of the negative photoresist SU-8 (micro resist technology GmbH) on a 4 in. silicon wafer, each layer exposed to near UV (EVG 620, EV Group) through a separate transparency mask. These masks were designed in AutoCAD 2015 (Autodesk) and printed on transparencies using a high-resolution printer (CAD/Art (Oregon, USA)). The first 25 µm thick layer of photoresist (SU-8 3025) was exposed through a mask with the full device design being transparent. The second 10 µm thick layer (SU-8 3005) was exposed through a similar mask, but with the two channels that connect the feed of the dispersed phases to the chambers of the DoD generators (i.e., the nozzles) made non-transparent in order to keep the nozzle height 25 µm. The third 5 µm thick layer (SU-8 3005) was exposed through a mask that featured transparent chambers of the DoD generators in order to increase their height to 40 µm and the guiding rail that then becomes 5 µm high. The three masks were provided as an AutoCAD file in the Supporting Information. After spin-coating, each layer was soft baked, exposed, and post-exposure baked, following the guidelines provided by the manufacturer. After the post-exposure bake of the third layer, the wafer was developed with mr-Dev 600 (micro resist technology GmbH) to dissolve the uncured photoresist, washed with isopropyl alcohol (IPA) and spin-dried. The resulting wafer was hard-baked for 30 min at 150 °C, and gradually cooled down on a heating plate to avoid cracks in the resulting SU-8 structures. Before using the

wafer as a master for creating PDMS stamps, its surface was silanized by exposing it to vapors of 1H,1H,2H,2H-perfluorooctyl-trichlorosilane in a depressurized desiccator.

PDMS devices were prepared by mixing 80 g of PDMS elastomer and 8 g of curing agent (Dow corning, Slygard 184 elastomer kit). The mixture was degassed and poured over the master placed in a 5 in. petridish. After 4 h in the oven at 70 °C for 4 h, cured PDMS was carefully peeled off from the wafer and cut to size. Inlets were punched with a 0.75 mm biopsy punch (Rapid core) and the outlet with a 1.5 mm biopsy punch (Rapid core). The PDMS stamps were then washed with ethanol and IPA to remove dust and debris. The stamps were covalently bonded to PDMS spin coated glass slides (25 mm × 75 mm) after exposing them to an oxygen plasma (Harrick, PDC-002) for 140 s at a pressure of 0.2–0.4 mbar. The obtained microfluidic devices were then baked at 200 °C for at least 4 h to recover the hydrophobicity of PDMS. A small piece of PTFE tubing (0.3 mm ID, 1/16 inch OD, 1 cm in length, Kinesis) was inserted into the outlet and glued tightly. Stainless steel connectors (0.025 in. OD × 0.013 in. ID, 23 g Elveflow) were inserted into all four inlets and glued tightly with water resistant glue. Finally, the microfluidic chips were soaked in demineralized water for a week in a covered petridish to saturate the PDMS matrix with water. This is an important step in order to reduce evaporation of water through PDMS, which leads to shrinkage of droplets in long-term cell growth experiments.

Experimental Setup: A commercially available pressure-based flow controller (MFCS-4C 1000 mbar/7000 mbar, Fluigent) was used to control the injection of fluids. The ports on this pressure controller were connected to reservoirs containing the fluids using silicone tubing and tightly sealed with parafilm. Soft walled Tygon tubing (0.02 in. ID, 1/16 in. OD, 50 cm in length) was used to connect the reservoirs to the metal connectors glued to the inlets of the chip. Care was taken to use the same height difference between the outlet of the chip and the liquid levels in the reservoirs in order to have comparable contributions of the hydrostatic pressure between different sets of experiments and use the provided MATLAB script (see Supporting Information). Relatively large reservoirs (15 mL centrifuge tubes) were used to ensure a negligible change in liquid level over the course of an experiment. Full details on the protocol to produce droplets on-demand, including a Matlab script, were provided in the authors' previous work.[37] Experiments to demonstrate the fluidic operations of the device (Figures 2 and 3) were carried out at room temperature and atmospheric pressure. On-chip cell growth experiments were carried out in an incubation system (Ibidi stage top incubator, Ibidi Gmbh) mounted on top of an inverted microscope (Axiovert S100, Zeiss). In order to avoid leakages and distortion during imaging utmost care was given while connecting the tubing from the fluid reservoirs to the microfluidic chip and fixing the chip inside the incubator box. The microfluidic chip was fixed on the bottom heated plate with temperature set point of 30 °C. The top plate temperature was also fixed at 30 °C. The incubation box was supplied with a gas mixture of 21 % O_2 and 79 % N_2, which was being saturated with water vapor through a humidifier bottle and flown through a tube with jacketed heater at 5.2 L h^{-1}. The humidity inside the box was maintained at 99 % to reduce water evaporation from the cell-containing droplet during the 24 h time lapse.

Image Acquisition and Analysis: Image acquisition was done using a TIS camera (DMK 33UJ003, The Imaging Source) mounted on a microscope using a combination of a 10× objective and a 0.63× mount objective. For the cell growth experiments, images were acquired at a frame rate of 5 frames per min for 24 h. The resolution obtained with this setup allowed single cells to be identified on the acquired images, see a close-up in Figure S3, Supporting Information. The images acquired to demonstrate the feeding capabilities (Figure 3) were processed to determine the length, L, and intensity, I, of the trapped droplet after each coalescence event using Fiji. The length was subsequently used to determine the droplet volume using $V = [hw - (4 - \pi)(2/h + 2/w)^{-2}](L - w/3)$, with h the height of the trap of 35 µm and w the width of the trap of 300 µm, see ref. [48] for further details. The intensity values were normalized with the intensity of the first incoming ink droplet I_{ink}. Quantification of cell growth experiments was performed by counting the number of cells in

**ADVANCED
SCIENCE NEWS**
www.advancedsciencenews.com

**ADVANCED
MATERIALS
TECHNOLOGIES**
www.advmattechnol.de

each image. Although this process could be automated, the cells were manually counted using a stylus for a selected number of images.

Working Fluids: The continuous phase used in all experiments is the fluorinated oil HFE-7500 (3M, Novec 7500 Engineered fluid) in which 0.05 v/v% Pico-Surf-1 (SphereFluidics) was dissolved in order to stabilize the interfaces and to ensure complete wetting of the PDMS walls ensuring controllable droplet operations. This oil is commonly used in cell experiments in microfluidic device and it was selected for its known compatibility with PDMS, high oxygen solubility, and biocompatibility.[49,50]

In the experiments that demonstrate the fluidic operations, demineralized water to produce the trapped and fed droplets in Figure 2 was used and brilliant blue dye (0.1 w/w%) was added to produce the reagent droplets in Figure 3 as a means to quantify the amount of reagents fed. In the cell growth experiments, cell-containing droplets were produced from a solution of *C. jadinii* cells in defined media with a glucose concentration of 2 g L^{-1}. The protocol used to prepare this solution, including the protocol for the preculturing step and the preparation of the defined media itself is provided below. Nutrient droplets were produced from defined media, with glucose concentrations in the range between 0.1 and 5.0 g L^{-1}.

Finally, a 5 v/v % solution of PFO (1H, 1H, 2H, 2H - perfluoro-1-octanol, Sigma-Aldrich) in HFE-7500 was used to induce coalescence. PFO was selected as it is well-known to break emulsions of cell-containing droplets,[51] and considered its cytotoxicity when selecting its concentration (see Figure S4, Supporting Information). 2,2,3,3,4,4,-Hepta-fluroButanol (Sigma-Aldrich) used in previous work was also considered to chemically induce droplet coalescence,[52] but was found to be cytotoxic at concentrations required for efficient coalescence.

Preparation of the Solution of Cyberlindnera (Pichia) Jadinii Cells in Defined Media: *C. jadinii* cells (CBS621) were obtained from the collection of the Westerdijk Fungal Biodiversity Institute, Utrecht, the Netherlands. A cell stock was prepared in 2 mL cryovials containing YPD and glycerol and stored at −80 °C. For every growth experiment, a fresh cryovial was taken from the stock.

After thawing at room temperature, 50 µL of cell solution was pipetted from the cryovial and inoculated into 5 mL of YPD (Yeast–Peptone–Dextrous) preculture medium. This medium was prepared by thoroughly mixing 20 g L^{-1} of glucose (Sigma-Aldrich), 10 g L^{-1} of yeast extract (Sigma-Aldrich), and 20 g L^{-1} of bacteriological peptone (Sigma-Aldrich) in a desired amount of demineralized water and subsequently sterilizing it by pushing the solution through a 0.2 µm syringe filter (Whatman). The inoculation was done in an autoclaved round bottom flask of 50 mL. Cotton wool was used to cover the flask to maintain aseptic conditions, while ensuring sufficient aeration. The flask was incubated overnight for 16 h in an orbital shaker at 30 °C and 190 rpm.

The precultured cell-YPD solution was centrifuged to remove the supernatant and then washed three times with defined media (see preparation protocol below). For the two sets of experiments with about 10 and about 40 cells inside the initial droplet, 2 and 4 mL of the precultured cell-YPD solution were respectively used and washed with defined medium to obtain 10 mL of the final cell solution with defined medium. 200 µL of fresh YPD was pipetted to the obtained solutions to boost the growth of cells inside the microfluidic chip. The resulting cell solution in defined media was transferred to a 15 mL centrifuge tube and stored at 30 °C in an incubator for at most 30 min prior to connecting the reservoir to the pressure pump to start the microfluidic experiments.

The defined medium was prepared by mixing 2.3 g L^{-1} of urea (CO(NH$_2$)$_2$, Sigma-Aldrich), 10 g L^{-1} of magnesium sulphate heptahydrate (MgSO$_4$.7H$_2$O, Sigma-Aldrich), 3 g L^{-1} of potassium hydrogen phosphate (KH$_2$PO$_4$, Sigma-Aldrich) and the desired concentration of glucose (0.1 to 5 g L^{-1}) in demineralized water. All components were weighed according to the desired final weight of the solution and the solution was mixed thoroughly. Then 1 mL L^{-1} of trace element solution and 1 mL L^{-1} of vitamin solution was added, see Tables S1 and S2, Supporting Information for their preparation protocols. The pH value was subsequently adjusted to 6.0 with a 2 M KOH solution and demineralized water was added again to reach the final weight. The

prepared medium was then filter sterilized by pushing it from a 50 mL syringe through a 0.2 µm syringe filter (Whatman) into a sterile bottle or tube. The obtained defined media was stored in a laminar flow cabinet until being used to prepare the cell-containing solution (with 2 g L^{-1} of glucose) or as the nutrient solution (with 0.1, 0.2, 1.0, 2.0, or 5.0 g L^{-1} of glucose).

Microbial Growth Model: In order to design and interpret the experiments, a simple theoretical cell growth model was used. As detailed in the Supporting Information, the amount of biomass *X* (in g) and the glucose concentration C_s (in g L^{-1}) in the droplet of volume *V* (in L) were described by the following set of coupled differential equations:

$$\frac{dX}{dt} = Y_{x/s}\left(q_{s,max}\left(\frac{C_s}{K_s + C_s}\right) - m_s\right)X \qquad (1)$$

and

$$\frac{dC_sV}{dt} = -q_{s,max}\left(\frac{C_s}{K_s + C_s}\right)X \qquad (2)$$

with $Y_{x/s}$ (biomass yield on glucose), $q_{s,\,max}$ (maximum specific uptake rate), K_s (affinity constant), and m_s (maintenance coefficient) as the four model parameters specific to the here cultured *C. jadinii* cells under the here cultured conditions. For the design of the experiments, the following estimates were used based on literature: $Y_{x/s}$ = 0.51 gX/gS,[53] $q_{s,\,max}$ = 1.25 h^{-1},[41] K_s = 0.36 g L^{-1}[42] and m_s = 0.01 gS/(gX h) (value reported for *Saccharomyces cerevisiae* [54]). For the interpretation of the data in Figure 6, the same values for K_s and m_s were used, while using $Y_{x/s}$ and $q_{s,\,max}$ as fit parameters, see the Supporting Information for details. As it is more common to report the maximum growth rate, μ_{max}, it was computed from the obtained values as explained in the Supporting Information.

To convert biomass *X* (in grams) into cell number *N*, $N = X/m_{cell}$ where m_{cell} is the mass of single cell was used and estimated as follows: first, the average volumes of 15 cells were determined to obtain 80.2 µm^3. Second, the wet cell mass was calculated to be 88 pg based on a specific gravity of 1.1 commonly reported for yeast.[55,56] Third, the dry cell mass was determined to obtain m_{cell} = 22 pg using the approximation that dry matter comprises about a quarter of the wet cell mass.[57,58]

Supporting Information

Supporting Information is available from the Wiley Online Library or from the author.

Acknowledgements

Conflict of Interest

The authors declare no conflict of interest.

Author Contributions

K.T., V.v.S., and W.M.v.G. designed the experiments. K.T. and Y.C.W. performed the experiments. Y.C.W. performed the modeling to compare with the experiments. K.T. and T.d.R. developed the droplet on-demand

**ADVANCED
SCIENCE NEWS**

www.advancedsciencenews.com

**ADVANCED
MATERIALS
TECHNOLOGIES**

www.advmattechnol.de

[1] S. Parekh, V. Vinci, R. Strobel, *Appl. Microbiol. Biotechnol.* **2000**, *54*, 287.

[2] B. S. Kim, S. C. Lee, S. Y. Lee, Y. K. Chang, H. N. Chang, *Bioprocess Biosyst. Eng.* **2004**, *26*, 147.

[3] G. Larsson, S. Jørgensen, M. Pons, B. Sonnleitner, A. Tijsterman, *J. Biotechnol.* **1997**, *59*, 3.

[4] G. W. Luli, W. R. Strohl, *Appl. Environ. Microbiol.* **1990**, *56*, 1004.

[5] M. Scheidle, M. Jeude, B. Dittrich, S. Denter, F. Kensy, M. Suckow, D. Klee, J. Büchs, *FEMS Yeast Res.* **2009**, *10*, 83.

[6] C. Stöckmann, M. Scheidle, B. Dittrich, A. Merckelbach, G. Hehmann, G. Melmer, D. Klee, J. Büchs, H. A. Kang, G. Gellissen, *Microb. Cell Fact.* **2009**, *8*, 22.

[7] P. Neubauer, N. Cruz, F. Glauche, S. Junne, A. Knepper, M. Raven, *Eng. Life Sci.* **2013**, *13*, 224.

[8] M. Jeude, B. Dittrich, H. Niederschulte, T. Anderlei, C. Knocke, D. Klee, J. Büchs, *Biotechnol. Bioeng.* **2006**, *95*, 433.

[9] T. Keil, B. Dittrich, C. Lattermann, T. Habicher, J. Büchs, *J. Biol. Eng.* **2019**, *13*, 18.

[10] T. Habicher, V. Czotscher, T. Klein, A. Daub, T. Keil, J. Büchs, *Biotechnol. Bioeng.* **2019**, *116*, 2250.

[11] A. Buchenauer, M. Hofmann, M. Funke, J. Büchs, W. Mokwa, U. Schnakenberg, *Biosens. Bioelectron.* **2009**, *24*, 1411.

[12] M. Funke, A. Buchenauer, W. Mokwa, S. Kluge, L. Hein, C. Müller, F. Kensy, J. Büchs, *Microb. Cell Fact.* **2010**, *9*, 86.

[13] M. Funke, A. Buchenauer, U. Schnakenberg, W. Mokwa, S. Diederichs, A. Mertens, C. Müller, F. Kensy, J. Büchs, *Biotechnol. Bioeng.* **2010**, *107*, 497.

[14] A. Groisman, C. Lobo, H. Cho, J. K. Campbell, Y. S. Dufour, A. M. Stevens, A. Levchenko, *Nat. Methods* **2005**, *2*, 685.

[15] F. K. Balagaddé, L. You, C. L. Hansen, F. H. Arnold, S. R. Quake, *Science* **2005**, *309*, 137.

[16] Z. Zhang, P. Boccazzi, H.-G. Choi, G. Perozziello, A. J. Sinskey, K. F. Jensen, *Lab Chip* **2006**, *6*, 906.

[17] S. H. Au, S. C. Shih, A. R. Wheeler, *Biomed. Microdevices* **2011**, *13*, 41.

[18] W. Du, L. Li, K. P. Nichols, R. F. Ismagilov, *Lab Chip* **2009**, *9*, 2286.

[19] D. V. Zhukov, E. M. Khorosheva, T. Khazaei, W. Du, D. A. Selck, A. A. Shishkin, R. F. Ismagilov, *Lab Chip* **2019**, *19*, 3200.

[20] A. Grünberger, W. Wiechert, D. Kohlheyer, *Curr. Opin. Biotechnol.* **2014**, *29*, 15.

[21] S. Täuber, E. von Lieres, A. Grünberger, *Small* **2020**, *16*, 1906670.

[22] A. Burmeister, A. Grünberger, *Curr. Opin. Biotechnol.* **2020**, *62*, 106.

[23] G. J. Nossal, J. Lederberg, *Nature* **1958**, *181*, 1419.

[24] B. Rotman, *Proc. Natl. Acad. Sci. USA* **1961**, *47*, 1981.

[25] E. M. Payne, D. A. Holland-Moritz, S. Sun, R. T. Kennedy, *Lab Chip* **2020**, *20*, 2247.

[26] T. Kaminski, P. Garstecki, *Chem. Soc. Rev.* **2017**, *46*, 6210.

[27] T. S. Kaminski, O. Scheler, P. Garstecki, *Lab Chip* **2016**, *16*, 2168.

[28] J. J. Agresti, E. Antipov, A. R. Abate, K. Ahn, A. C. Rowat, J.-C. Baret, M. Marquez, A. M. Klibanov, A. D. Griffiths, D. A. Weitz, *Proc. Natl. Acad. Sci. USA* **2010**, *107*, 4004.

[29] B. L. Wang, A. Ghaderi, H. Zhou, J. Agresti, D. A. Weitz, G. R. Fink, G. Stephanopoulos, *Nat. Biotechnol.* **2014**, *32*, 473.

[30] T. Beneyton, I. P. M. Wijaya, P. Postros, M. Najah, P. Leblond, A. Couvent, E. Mayot, A. D. Griffiths, A. Drevelle, *Sci. Rep.* **2016**, *6*, 27223.

[31] K. Leung, H. Zahn, T. Leaver, K. M. Konwar, N. W. Hanson, A. P. Pagé, C.-C. Lo, P. S. Chain, S. J. Hallam, C. L. Hansen, *Proc. Natl. Acad. Sci. USA* **2012**, *109*, 7665.

[32] M. Hébert, M. Courtney, C. L. Ren, *Lab Chip* **2019**, *19*, 1490.

[33] S. H. Jin, H.-H. Jeong, B. Lee, S. S. Lee, C.-S. Lee, *Lab Chip* **2015**, *15*, 3677.

[34] S. Jakiela, T. S. Kaminski, O. Cybulski, D. B. Weibel, P. Garstecki, *Angew. Chem., Int. Ed.* **2013**, *52*, 8908.

[35] X. Jian, X. Guo, J. Wang, Z. L. Tan, X.-h. Xing, L. Wang, C. Zhang, *Biotechnol. Bioeng.* **2020**, *117*, 1724.

[36] R. F.-X. Tomasi, S. Sart, T. Champetier, C. N. Baroud, *Cell Rep.* **2020**, *31*, 107670.

[37] K. Totlani, J.-W. Hurkmans, W. M. van Gulik, M. T. Kreutzer, V. van Steijn, *Lab Chip* **2020**, *20*, 1398.

[38] W. Visser, W. A. Scheffers, W. H. Batenburg-van der Vegte, J. P. van Dijken, *Appl. Environ. Microbiol.* **1990**, *56*, 3785.

[39] J.-u. Shim, G. Cristobal, D. R. Link, T. Thorsen, Y. Jia, K. Piattelli, S. Fraden, *J. Am. Chem. Soc.* **2007**, *129*, 8825.

[40] A. Dewan, J. Kim, R. H. McLean, S. A. Vanapalli, M. N. Karim, *Biotechnol. Bioeng.* **2012**, *109*, 2987.

[41] E. Postma, A. Kuiper, W. Tomasouw, W. Scheffers, J. Van Dijken, *Appl. Environ. Microbiol.* **1989**, *55*, 3214.

[42] E. Postma, W. A. Scheffers, J. P. Van Dijken, *Microbiology* **1988**, *134*, 1109.

[43] C. Verduyn, A. H. Stouthamer, W. A. Scheffers, J. P. van Dijken, *Antonie Van Leeuwenhoek* **1991**, *59*, 49.

[44] M. Tobajas, E. Garcia-Calvo, *World J. Microbiol. Biotechnol.* **1999**, *15*, 431.

[45] M. Imura, K. Nitta, R. Iwakiri, F. Matsuda, H. Shimizu, E. Fukusaki, *J. Biosci. Bioeng.* **2020**, *129*, 52.

[46] V. Ortseifen, M. Viefhues, L. Wobbe, A. Grünberger, *Front. Bioeng. Biotechnol.* **2020**, *8*, 1324.

[47] Y. Xia, G. M. Whitesides, *Annu. Rev. Mater. Sci.* **1998**, *28*, 153.

[48] M. Musterd, V. van Steijn, C. R. Kleijn, M. T. Kreutzer, *RSC Adv.* **2015**, *5*, 16042.

[49] P. Gruner, B. Riechers, L. A. C. Orellana, Q. Brosseau, F. Maes, T. Beneyton, D. Pekin, J.-C. Baret, *Curr. Opin. Colloid Interface Sci.* **2015**, *20*, 183.

[50] J.-C. Baret, *Lab Chip* **2012**, *12*, 422.

[51] L. Mazutis, J. Gilbert, W. L. Ung, D. A. Weitz, A. D. Griffiths, J. A. Heyman, *Nat. Protoc.* **2013**, *8*, 870.

[52] I. Akartuna, D. M. Aubrecht, T. E. Kodger, D. A. Weitz, *Lab Chip* **2015**, *15*, 1140.

[53] E. Hernandez, M. J. Johnson, *J. Bacteriol.* **1967**, *94*, 996.

[54] T. Vos, X. D. Hakkaart, E. A. de Hulster, A. J. van Maris, J. T. Pronk, P. Daran-Lapujade, *Microb. Cell Fact.* **2016**, *15*, 111.

[55] A. K. Bryan, A. Goranov, A. Amon, S. R. Manalis, *Proc. Natl. Acad. Sci. USA* **2010**, *107*, 999.

[56] S. A. Haddad, C. C. Lindegren, *Appl. Microbiol.* **1953**, *1*, 153.

[57] A. Schmid, H. Kortmann, P. S. Dittrich, L. M. Blank, *Curr. Opin. Biotechnol.* **2010**, *21*, 12.

[58] F. Sherman, in *Methods in Enzymology* (Eds: J. Abelson, M. Simon, G. Verdine, A. Pyle), vol. *350*, Academic Press, Cambridge, MA **2002**, pp. 3–41.